Available online at www.sciencedirect.com
ScienceDirect
Ceramics International 34 (2008) 1473–1480
CERAMICS INTERNATIONAL
www.elsevier.com/locate/ceramint

Studies on the microstructure of the black-glazed bowl sherds excavated from the Jian kiln site of ancient China

Weidong Li [a,*], Hongjie Luo [a], Jianan Li [b], Jiazhi Li [a], Jingkun Guo [a]

[a] *Shanghai Institute of Ceramics, Chinese Academy of Sciences, Shanghai 200050, China*
[b] *The Museum of Fujian Province, Fuzhou, Fujian 350001, China*

Received 14 February 2007; received in revised form 19 February 2007; accepted 2 April 2007
Available online 3 May 2007

Abstract

The Jian kiln, located in present-day Jianyang county of Fujian province, mainly produced black-glazed tea bowls. Jian tea bowl was used as a utensil for tea tasting and was greatly appreciated by emperor Huizong of the Northern Song dynasty. The black glaze of Jian bowl was sometimes marked with streaks or spots, usually called ‘‘hare's fur'' or ‘‘oil spot'', which are the crystalline markings of iron oxide precipitated during firing in the dragon kiln. In this study, black-glazed Jian bowl sherds excavated from the late Northern Song strata of Luhuaping and Daluhoumen Jian kiln sites were adopted as test samples. Based on the physico-chemical foundation for the formation of glaze microstructure, the correlation among composition, microstructure, and visual appearance has been investigated by means of energy-dispersive X-ray fluorescence, X-ray diffraction, and field emission electron microscopy. For the first time, the study provides realizing proofs for two kinds of microstructural forming mechanics.

Keywords: Jian kiln; Black-glazed tea bowl; Microstructure; Crystallization

1. Introduction

The Jian kiln is located in present-day Jianyang county of Fuian province, which originally produced green-glazed wares in the Tang dynasty (618–907 A.D.) It was not until the Song dynasty (960–1279 A.D.), a time when the values of a cultivated scholar class guided taste as never before, that the Jian kiln began to make the famous black-glazed tea bowls until it closed down in the Yuan dynasty (1279–1368 A.D.) [1]. Black-glazed Jian tea bowls were perfect for highlighting the rich white tea decoction. The thick and lustrous black glaze of Jian bowl sometimes featured streaked or mottled patterns, usually called ‘‘hare's fur'' or ‘‘oil spot'', which are the crystalline markings of iron oxide precipitated during firing in the dragon kiln. According to the book Da Guan Cha Lun, written by Song emperor Huizong (reigned 1100–1125), which has been cited frequently by other authors, ‘‘Those Jian tea bowls with a dark-blue or black color were of superior quality, especially those with jade-like streaks''. ‘‘Jade-like streak'' describes the hare's fur appearance [2]. Japanese Buddhist monks who visited temples in southern China brought back home the much-admired Jian bowls called in Japan as temmoku wares. The Yohen Temmoku ware with ‘‘sparkling'' oil spots conserved now in Japan is part of the national treasure of Japan. From 1960 to 1993, ten dragon kilns of the late Tang dynasty to the Yuan dynasty have been excavated, a large quantities of black-glazed bowls and kiln furniture have also been found in the Northern Song stratum and Southern Song stratum [1].

Since the manufacturing techniques were lost, the Jian bowl has been appraised as mysterious and costly treasure through the generations past. In the Song dynasty, potters of Jianyang were already proficient in firing Jian bowls, though they did not understand the inherent reasons behind the bowl appearance at that time of 1000 years ago. Some researchers have studied the chemistry and microstructure of Jian wares, giving a generally correct description of the phases present [2,3]. In this study, glaze formulation requirements were placed on a physico-chemical foundation. The glaze and body compositions and microstructures were studied by means of EDXRF, XRD, FESEM/EDS, aiming at investigating the correlation among composition, microstructure, firing technique and glaze

* Corresponding author. Tel.: +86 21 52412373; fax: +86 21 52413903.
E-mail address: liwd@mail.sic.ac.cn (W. Li).

0272-8842/$34.00
doi:10.1016/j.ceramint.2007.04.004

appearance, disclosing the scientific rules behind the aesthetically pleasing appearance of Jian glazes.

2. Experimental

Twenty-three black-glazed bowl sherds J1–J23 excavated from the late Northern Song strata of Luhuaping and Daluhoumen sites, were provided by the museum of Fujian province. Glaze and body composition was examined by energy-dispersive X-ray fluorescence (EDAX Eagle-IIIμProbe, USA). X-ray diffraction (D/max 2550 V, Japan) using Cu Kα radiation was employed to identify the crystalline phases in glaze. Glaze maturing range was estimated according to the temperature interval between FP (flowing point) and HP (hemisphere point) measured using high temperature microscope (MHO-2, Germany). Microstructure and phase composition was studied using field emission electron microscopy (JSM-6700F, Japan) equipped with EDS and SAD. FESEM samples were obtained by etching polished cross sections of glazes in dilute HF solution at room temperature.

3. Results and discussion

3.1. Influence of chemical composition on the formation of microstructure

As shown in Table 1, the Jian glazes are attributed to high temperature iron oxide–kalia–calcia–magnesia–aluminosilicate glazes, which could be roughly represented with the SiO_2–Al_2O_3–CaO ternary system by merging MgO into CaO and ignoring Fe_2O_3 and K_2O. The overall glaze compositions of J1–J23 concentrate in the primary crystalline phase region of anorthite, possessing thermodynamic qualification for the crystallization of anorthite. It is not so simple to explain the crystallization behavior of the Jian glaze, because, the function of iron oxide in the glaze composition is quite complex and subtle. Iron oxide actually has a dual function, on one hand it acts as a flux, on the other hand iron ion favors the strong immiscibility tendency between SiO_2 and CaO and locates preferably in the phase enriched by CaO oxides with a large number of nonbridging oxygen atoms. Therefore, as a result of the compositional fluctuation of Fe_2O_3, Al_2O_3 and SiO_2 contents from one Jian glaze to another, the microstructure formation mechanism might cover three different cases, i.e. (1) crystallization of anorthite accompanied by inter-crystal phase separation and the subsequent crystallization of iron oxide; (2) local phase separation in glaze surface neighbouring area followed by crystallization of iron oxide; (3) homogeneous amorphous glaze without crystallization or phase separation.

The ceramic body compositions as shown in Table 2 have high alumina (17.46–23.14 wt.%), silica (63.35–71.91 wt.%), and especially high iron oxide (4.80–9.44 wt.%) contents.

Except pure black Jian glaze, in oil spot or hare's fur patterns forming processes, the crystallization of supersaturated iron oxides from glaze melt is a common character, among which the crystallization at the glaze surface/gas interface is the most frequently occurring situation. The mottled or streaked pattern on the Jian glaze turns out variations in shape, scale, distribution and color, closely associated with the variety, amount, integrity, and degree of order of the crystal precipitation on the glaze surface, which is determined by the firing techniques, the viscosity–temperature characteristic of glaze, and the process of bubble elimination. Bubble formation and elimination has a significant effect on the enrichment and distribution condition of iron. Thermal decomposition of Fe_2O_3 above 1230 °C within glaze and body is the main source of

Table 1
Major chemical compositions of glazes by EDXRF analysis (wt.%)

No.	Na_2O	MgO	Al_2O_3	SiO_2	P_2O_5	K_2O	CaO	TiO_2	MnO	Fe_2O_3
J1	0.24	2.91	17.14	62.72	0.44	3.52	8.22	0.32	0.48	3.93
J2	0.19	3.05	19.56	61.22	0.42	3.15	7.00	0.36	0.60	4.27
J3	0.61	2.29	19.08	62.99	0.33	2.85	5.92	0.40	0.47	5.42
J4	0.23	7.88	20.58	60.95	0.26	2.72	6.10	0.50	0.40	6.28
J5	0.20	1.68	18.11	64.51	0.32	2.84	4.96	0.40	0.46	6.42
J6	0.07	2.38	18.03	62.63	0.52	3.21	7.35	0.32	0.61	4.82
J7	0.52	2.40	17.21	62.29	0.38	3.05	7.83	0.35	0.50	5.38
J8	0.05	2.72	18.31	59.28	0.58	3.50	8.45	0.37	0.74	5.85
J9	0.06	2.80	18.38	61.37	0.47	3.28	6.66	0.33	0.80	5.39
J10	0.23	3.15	18.46	60.79	0.52	3.13	8.28	0.35	0.59	4.99
J11	0.26	1.78	12.20	68.75	0.15	2.38	3.80	0.37	0.36	3.53
J12	0.27	2.34	16.70	57.88	0.40	2.99	5.71	0.35	0.60	5.87
J13	0.07	2.42	17.34	64.21	0.42	3.15	6.02	0.39	0.80	4.73
J14	0.36	3.54	17.24	62.20	0.53	2.66	8.04	0.31	0.72	4.31
J15	0.26	2.43	17.62	64.08	0.46	3.04	6.67	0.29	0.62	4.43
J16	0.25	2.60	18.38	62.32	0.39	3.21	6.35	0.41	0.42	5.60
J17	0.37	2.67	17.74	62.94	0.41	2.32	6.55	0.35	0.44	6.12
J18	0.33	2.91	18.09	60.82	0.41	2.97	7.02	0.39	0.44	6.50
J19	0.31	2.24	17.41	64.50	0.32	2.80	5.56	0.34	0.54	5.89
J20	0.15	2.71	18.64	63.96	0.35	2.74	6.31	0.30	0.54	4.43
J21	0.31	1.50	13.87	59.77	0.29	2.04	5.88	0.30	0.60	6.26
J22	0.28	3.03	19.09	60.63	0.48	3.03	8.40	0.32	0.53	4.16
J23	0.27	2.59	19.80	61.53	0.40	3.25	5.86	0.37	0.56	5.29

Table 2
Major chemical compositions of bodies by EDXRF analysis (wt.%)

No.	Na_2O	MgO	Al_2O_3	SiO_2	K_2O	CaO	TiO_2	Fe_2O_3
J1	0.21	0.44	21.91	65.67	2.48	0.12	0.78	7.68
J2	0.15	0.75	20.08	70.51	2.43	0.30	0.83	4.80
J3	0.31	0.57	19.72	70.27	2.90	0.35	0.83	4.87
J4	0.31	1.19	19.8	66.63	2.36	0.88	0.72	7.83
J5	0.41	0.58	19.85	68.84	1.86	0.42	0.62	7.17
J6	0.36	0.57	21.27	66.77	2.46	0.65	0.65	7.2
J7	0.32	0.97	22.14	65.46	2.30	0.15	0.80	7.55
J8	0.18	0.72	23.14	64.67	2.48	0.12	0.78	7.68
J9	0.49	0.93	21.52	66.11	2.76	0.34	0.80	6.78
J10	0.26	0.75	17.46	71.91	2.10	0.17	0.76	6.29
J11	0.31	0.72	21.29	67.83	2.44	0.17	0.67	6.37
J12	0.38	1.06	21.62	65.23	2.74	0.2	0.93	7.57
J13	0.35	0.90	19.71	67.30	2.34	0.35	0.71	8.11
J14	0.18	0.72	21.10	68.51	2.06	0.30	0.78	6.12
J15	0.38	0.81	18.49	69.40	1.82	0.10	0.76	7.90
J16	0.54	0.90	21.93	65.61	2.30	0.12	0.75	7.55
J17	0.25	0.85	20.77	66.61	2.45	0.17	0.78	7.80
J18	0.39	0.74	22.62	63.39	2.12	0.11	0.88	9.44
J19	0.17	0.78	22.06	65.69	2.32	0.17	0.66	7.89
J20	0.36	0.54	22.31	65.35	2.68	0.10	0.88	7.57
J21	0.41	0.84	19.27	63.84	2.35	0.16	0.52	6.27
J22	0.39	0.63	20.70	68.40	2.67	0.44	0.53	6.02
J23	0.31	1.03	21.18	67.46	2.43	0.08	0.64	6.72

bubble generation. With the decomposition of Fe_2O_3, more and more iron would attach to the floating bubbles and go up to glaze surface adjacent area. Fig. 1 gives the backscattered SEM image of a bubble close to J6 glaze surface, clearly showing the light-colored iron-bearing particles enriched on the bubble wall.

According to high temperature microscope analysis, maturing range for the Jian glaze is 1300 ± 20 °C.

3.2. Outward appearance and crystalline phases of glaze

The outward appearances of the Jian bowl sherds observed with a stereo-microscope are listed in Table 3.

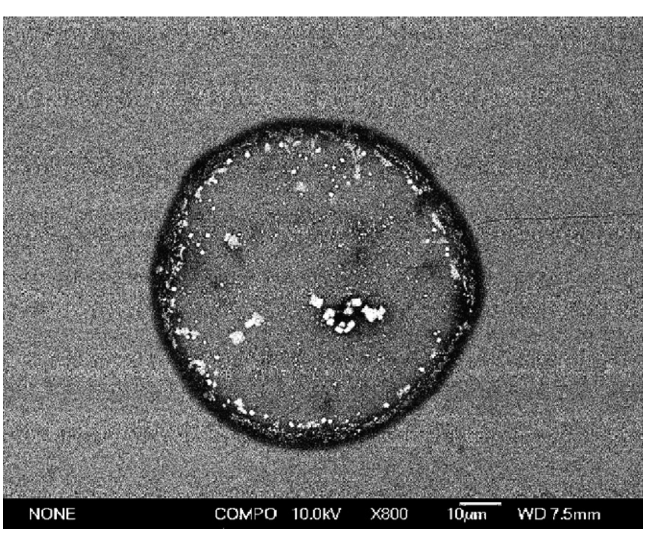

Fig. 1. A bubble close to J6 glaze surface, with iron oxide enriched on the bubble wall.

XRD analyses (Fig. 2) for J2 and J5 glaze surfaces show that the major phase present are anorthite with a small amount of maghemite (J2) and hematite (J5), while in J4 and J6 only ferrous oxide and hematite are present. Si, Ca and Al elements

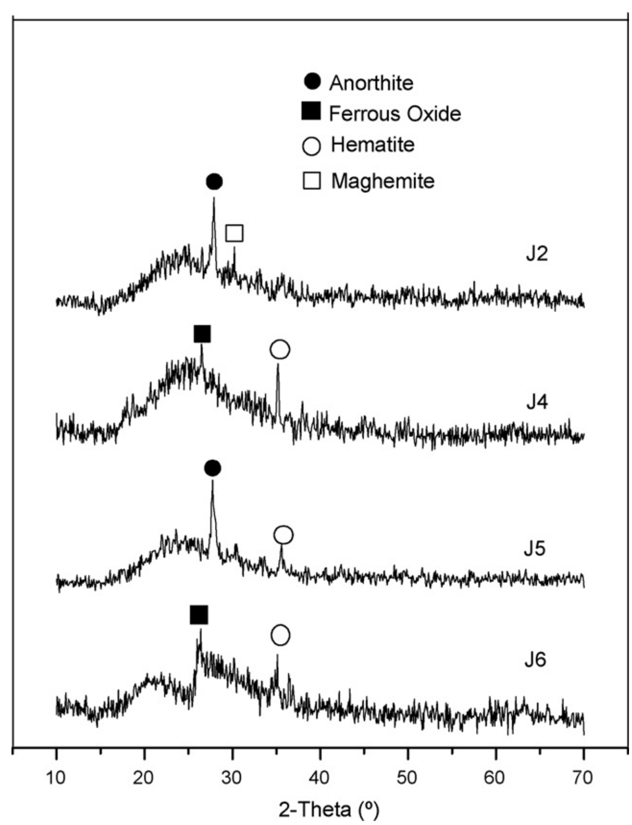

Fig. 2. XRD spectra of the glaze surfaces.

Table 3
Appearance description of the Black glazes from Jian kiln

No.	Glaze	Body
J2	Lustrous brown surface, yellow speckles	Grey body, bearing a few white quartz particles
J4	Lustrous black surface, silver-brown semi-lustrous stripes	
J5	Lustrous black surface, brown matte stripes	
J6	Lustrous black surface, yellowish-brown lustrous stripes	
J7	Lustrous black surface, silver-brown lustrous stripes	
J12	Matte brown surface	

are not concerned with surface crystallization. Therefore, an extrapolation can be inferred that J2 and J5 might accord with the mechanism of crystallization of anorthite accompanied by inter-crystal phase separation and the subsequent crystallization of iron oxide, while J4 and J6 might accord with the mechanism of local phase separation in glaze surface neighbouring area followed by crystallization of iron oxide. Further microstructure analyses will give proofs for the above inference.

3.3. Microstructure and its formation mechanism

Fig. 3 shows the microstructure of J5 glaze surface in the area of a stripe (hare's fur). From Fig. 3a, flower-shaped local crystallization zone of anorthite can be observed. In the interspaces of anorthite crystal clusters (marked as A and B in Fig. 3a–c) or the peripheral regions around crystals are accompanied by the general occurrence of liquid-liquid phase separation due to Al_2O_3 depletion. The white leafy crystals (marked as C in Fig. 3d) bordering around the anorthite flowers are related with the subsequent iron oxide crystallization from the phase-separated glass. Due to the severe Al_2O_3 depletion and high local iron contents from the purification effect of anorthite crystallization, the iron oxide crystal growth has developed well. The precipitation of small white snowflake-shaped iron oxide crystals on glaze surface can also be observed in A and B areas.

Fig. 4 provides a view of etched cross section of J5 in the position of a piece of hare's fur. Fig. 4a shows the aggregative clusters of anorthite precipitated from the glaze layer. Fig. 4b is a close-up of an anrthite cluster, edged by iron oxide precipitation. Fig. 4c is a close-up of zone A, the black isolated droplet is rich in silicon, while the white iron oxide crystal grain

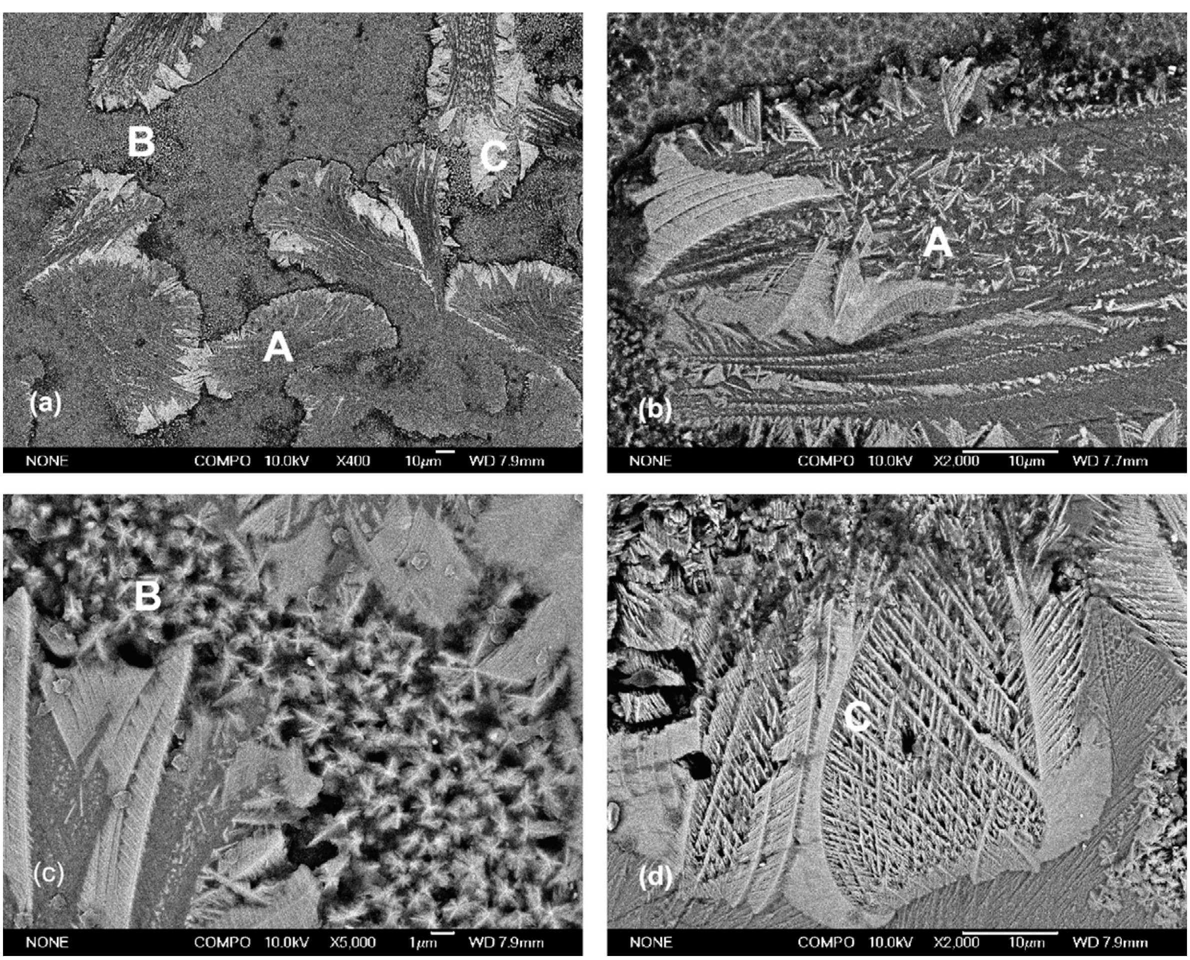

Fig. 3. Microstructure of the surface of black glaze J5 from Jian kiln.

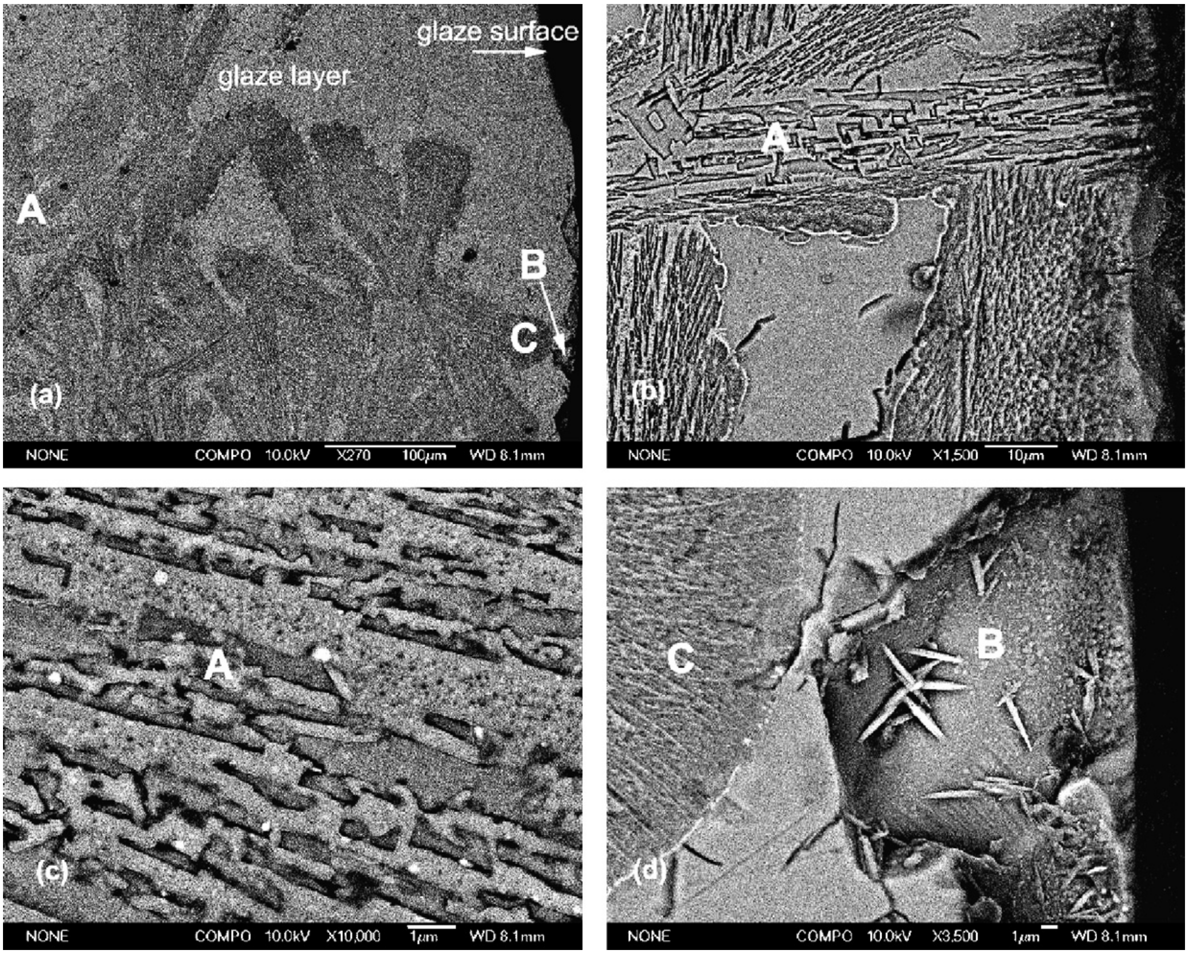

Fig. 4. Microstructure of the cross-section of black glaze J5 from Jian kiln.

which precipitates from the continuous phase is enriched in iron. Fig. 4d shows the shallow anorthite crystallization-phase separation zone beneath the glaze surface (zone C), resulting in superficial phase separation followed by further precipitation of iron oxide (Zone B). According to the above discussion, the forming mechanism of the microstructure of glaze J5 can be concluded as: bulk crystallization of anorthite develops within the glaze layer, with a small amount of anorthite revealed on the glaze surface. As the oxygen bubbles generated from the pyrolysis of Fe_2O_3 rise to the surface of the glaze, they will drag with them a bit of the anorthite and deposit it on the surface; the iron oxide enriched around the bubbles will also be carried to the surface, causing formation of the iron-rich area on the surface. During firing, the iron-enriched flux flows due to the low viscosity and the running streaks come into being. While cooling, iron oxide precipitates along the anorthite brim and in between anorthite crystals. Then the dull brown hare's fur effect can be observed. Within the glaze layer, the iron content of the inter-anorthite glass is relatively low, with small grainy iron oxide precipitated from the continuous iron-enriched phase.

Fig. 5 shows the microstructure of a cross section of J2 in the position of a piece of hare's fur. Fig. 5a and b clearly present the process of anorthite precipitation (gray, column or needle-shaped crystals) $\rightarrow$ inter-crystal phase separation (the dark isolated droplet is rich in SiO_2, the light continuous phase is rich in CaO and Fe_2O_3) $\rightarrow$ iron oxide precipitation (white grainy or dendritic crystal precipitates from the continuous phase). Fig. 5c and d shows the grainy iron oxide crystals arraying in a certain order. Fig. 5e presents the local phase separation zone resulting from the chemical heterogeneity. Fig. 5f is a close-up of Fig. 5e, showing three-dimensional interconnected phase separation structure.

Fig. 6 gives the microstructure of glaze J6. In Fig. 6a, J6 shows bright yellow-brown hare's fur (namely golden hare's fur) with 0.8–1.5 mm in width. As in Fig. 6b, snowflake shaped iron oxide crystal spreads all over the hare's fur (zone 1). The iron concentration of the black glaze between two furs is lower than that within the fur, and smaller iron oxide crystals can be observed indistinctly beneath the glaze surface (zone 2). Fig. 6c is an overhead view of a fur on the glaze surface. It can be seen that snowflake-shaped iron oxide precipitates in a very good order, piling up parallely with the glaze surface, layer upon layer, forming shining reflective streaks above the surface. Fig. 6d is a close-up of Fig. 6c, it can be seen more clearly that iron oxide precipitates on the glaze surface, fully

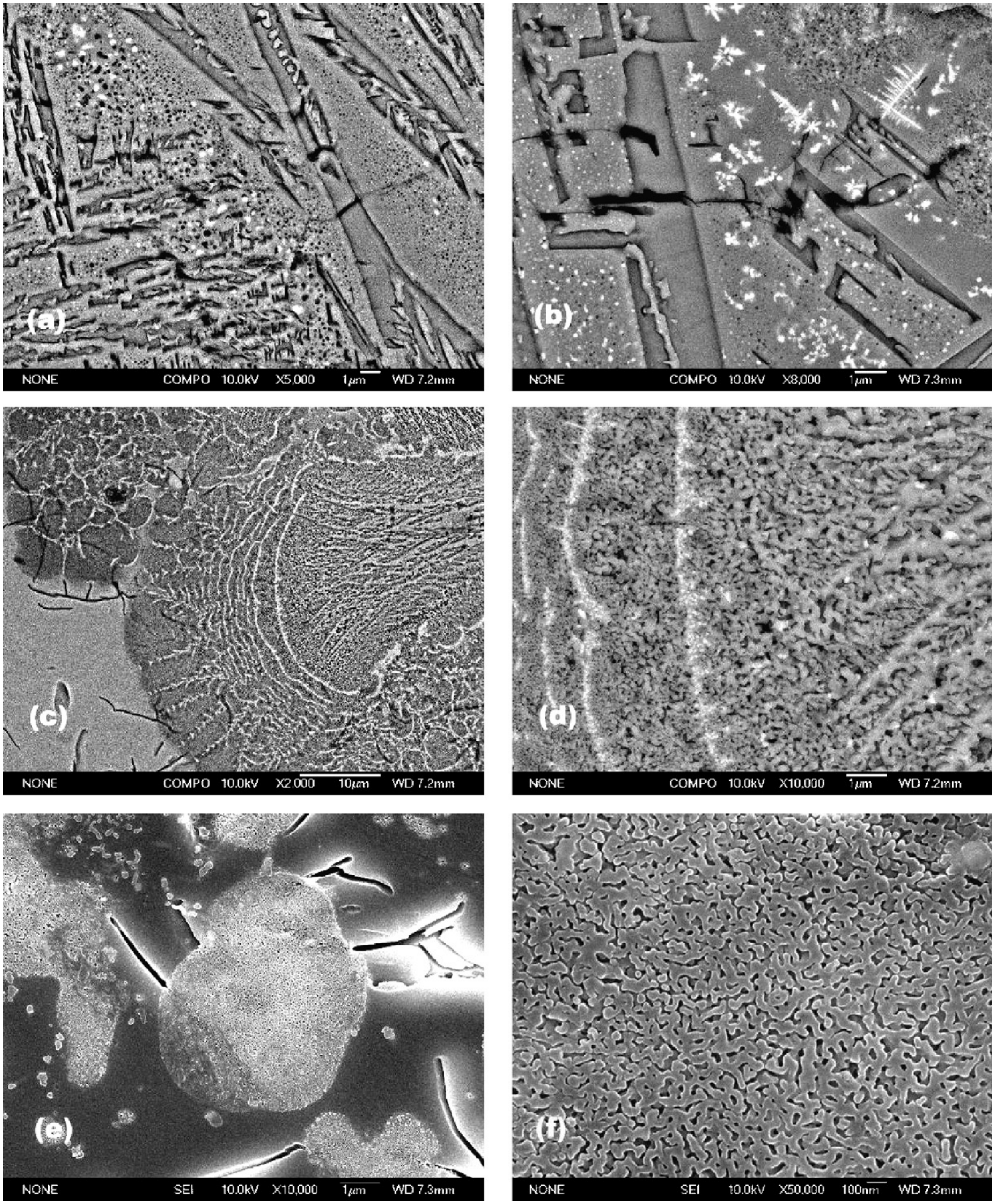

Fig. 5. Microstructure of the cross-section of black glaze J2 from Jian kiln.

develops and arrays in good order. Fig. 6e shows the cross section of glaze J6 in the position of a piece of hare's fur. Zone A is the directional surface crystallization layer of iron oxide with 2.0–2.5 μm in thickness. Zone B is the under-glaze phase separation area, in which the iron-rich phase provides iron for surface crystallization. Zone C is the phase separation-crystallization area within glaze, in which the white grain is the smaller iron crystals precipitated from the iron-rich phase owing to iron-supersaturation during cooling. Fig. 6f is a close-up of Fig. 6e. According to the above discussion, the forming mechanism of the microstructure of glaze J6 can be concluded that as temperature rises to over 1260 °C, the pyrolysis of Fe_2O_3 from body and glaze becomes more strenuous, setting more free bubbles. The bubbles rise, inflate gradually, merge and grow up. More and more iron oxide would be enriched around the bubbles. The iron-rich areas will form on the glaze surface after the ultimate release of bubble. During firing, the iron-enriched flux flows due to the low

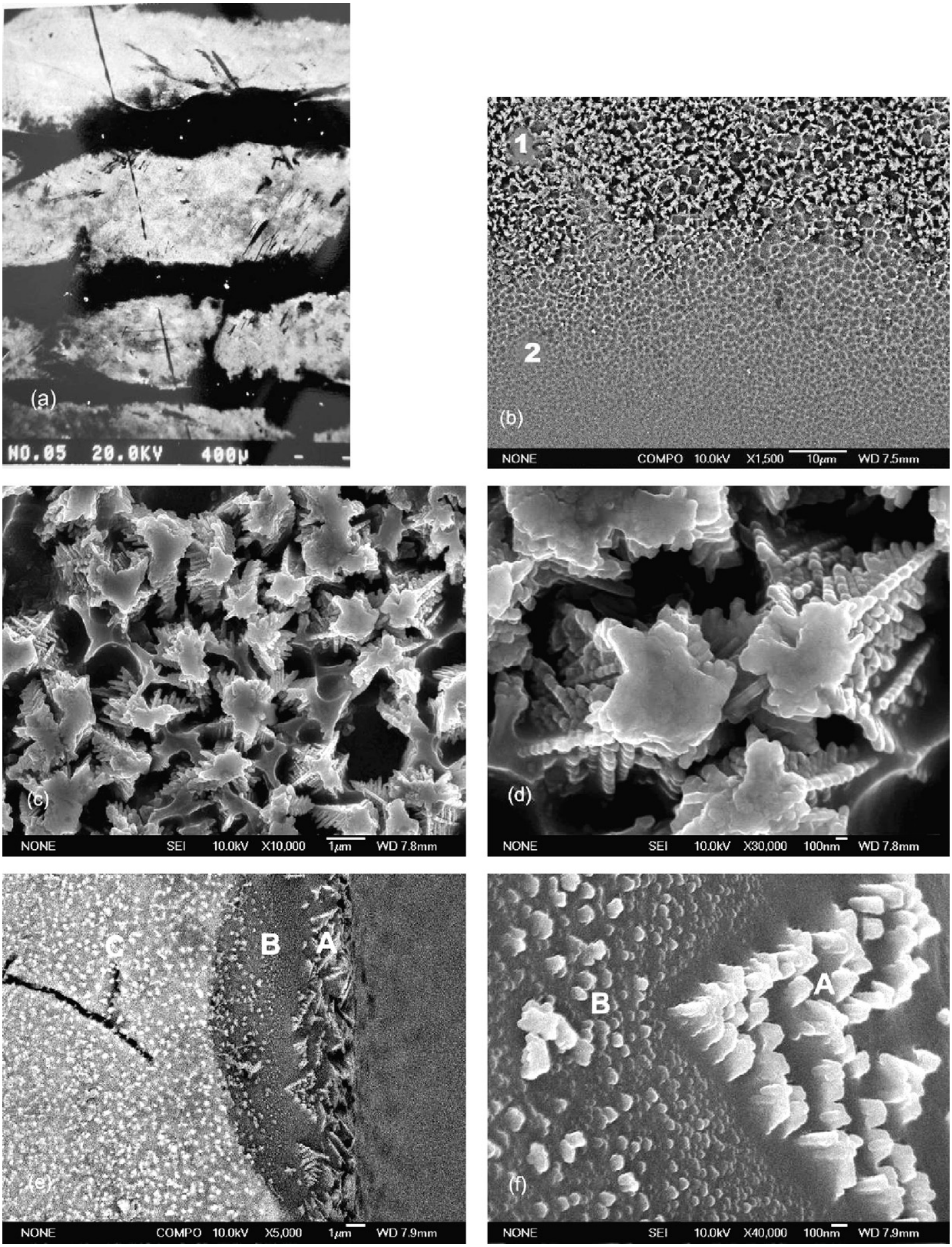

Fig. 6. Microstructure of black glaze J6 from Jian kiln.

viscosity and the running streaks come into being. While cooling, iron oxide would precipitate from the iron-rich continuous phase. The directional iron oxide precipitation on the surface turns out as yellow-brown sparkling hare's fur. Smaller iron oxide crystals precipitate within the glaze layer.

4. Conclusion

Jian glazes are attributed to high temperature calcia-iron oxide-aluminosilicate glazes. Iron oxide acts as both flux and phase-separation accelerator during firing, which actually plays a key role in the formation of the glaze microstructure. For the first time, this study provides convincing proofs for two kinds of microstructural forming mechanics, namely local phase separation in glaze surface neighbouring area followed by crystallization of iron oxide, and crystallization of anorthite accompanied by inter-crystal phase separation and the subsequent crystallization of iron oxide.

Acknowledgment

This work was supported by National Natural Science Foundation of China 50672119 and 50432010.

References

[1] Z. Fan, Archaeological Conspectus on the Ceramics from Fujian Province, Fujian Map Publishing Company, Fujian, 2001.
[2] J.-Z. Li, (Eds.), Science and Technology History of China, Vol. Ceramics, Science Publishing Company, Beijing, 1998.
[3] Z.-D. Lin, Pilot study on the black-glazed wares of ancient China, J. Chin. Ceram. Soc. 7 (3) (1979) 190–200.